The Journal of Immunology

PIKfyve, a Class III Lipid Kinase, Is Required for TLR-Induced Type I IFN Production via Modulation of ATF3

Xinming Cai, Yongyao Xu, You-Me Kim, Joseph Loureiro and Qian Huang

J Immunol 2014; 192:3383-3389; Prepublished online 5 March 2014;
doi: 10.4049/jimmunol.1302411
http://www.jimmunol.org/content/192/7/3383

The Journal of Immunology is published twice each month by
The American Association of Immunologists, Inc.,
1451 Rockville Pike, Suite 650, Rockville, MD 20852

Print ISSN: 0022-1767 Online ISSN: 1550-6606.

PIKfyve, a Class III Lipid Kinase, Is Required for TLR-Induced Type I IFN Production via Modulation of ATF3

Xinming Cai, Yongyao Xu, You-Me Kim,[1] Joseph Loureiro, and Qian Huang

Type I IFN plays a key role in antiviral responses. It also has been shown that deregulation of type I IFN expression following abnormal activation of TLRs contributes to the pathogenesis of systemic lupus erythematosus. In this study, we find that PIKfyve, a class III lipid kinase, is required for endolysosomal TLR-induced expression of type I IFN in mouse and human cells. PIKfyve binds to phosphatidylinositol 3-phosphate and synthesizes phosphatidylinositol 3,5-bisphosphate, and plays a critical role in endolysosomal trafficking. However, PIKfyve modulates type I IFN production via mechanisms independent of receptor and ligand trafficking in endolysosomes. Instead, pharmacological or genetic inactivation of PIKfyve rapidly induces expression of the transcription repressor ATF3, which is necessary and sufficient for suppression of type I IFN expression by binding to its promoter and blocking its transcription. Thus, we have uncovered a novel phosphoinositide-mediated regulatory mechanism that controls TLR-mediated induction of type I IFN, which may provide a new therapeutic indication for the PIKfyve inhibitor. ***The Journal of Immunology*****, 2014, 192: 3383–3389.**

Toll-like receptor signaling plays a critical role in the innate immune response. TLR pathways are triggered by pathogen-associated molecular patterns and coordinate inflammatory and antipathogen responses (1). It is known that dysregulated TLR signaling functions in a number of autoimmune diseases primarily caused by dysregulation of cytokine production (2). IFN-α, a member of the type I IFN family, induces many clinical features of SLE. An important source of IFN-α in vivo consists of plasmacytoid dendritic cells (pDCs) activated via TLR7 and TLR9 (3, 4). Within the TLR family of proteins, TLR7 recognizes ssRNA of viral origin, whereas TLR9 is a sensor for unmethylated CpG dinucleotides in viral and bacterial DNA. These TLR7 and TLR9 ligands traffic through early endosomes and are retained within endolysosomes. Newly synthesized TLR7 and TLR9 reside within the endoplasmic reticulum (ER) and are delivered to endolysosomal compartments upon activation (5, 6). This differential, activation-dependent receptor/ligand localization helps coordinate a proper response to pathogen-derived components yet avoids inappropriate responses to self-antigens. However, in lupus patients, immune complexes consisting of dsDNA from apoptotic cells and antinucleotide IgG are taken up by pDCs. This internalized immune complex activates the endosomal TLR7 and TLR9 pathway, leading to production of IFN-α and the progression of SLE (7).

PIKfyve is a class III lipid kinase that phosphorylates the D-5 position in endosomal phosphatidylinositol 3-phosphate [P1(3)P] to yield phosphatidylinositol 3,5-bisphosphate [$PI(3,5)P_2$] (8). Vac14 and Sac3 form a regulatory complex with PIKfyve. Both Vac14 and Sac3 are required for maximal PIKfyve activity (9–11). PIKfyve-mediated $PI(3,5)P_2$ signaling has been shown to play a critical role in multiple biological processes by regulating endosomal trafficking, such as GLUT4 translocation, retroviral budding (12, 13), autophagy (14), and neurodegeneration. Recently, we revealed that PIKfyve is the molecular target of apilimod (15), which is the first clinically evaluated small-molecule IL-12/IL-23 antagonist (16, 17). We have shown that apilimod specifically binds to PIKfyve and inhibits its activity, which in turn silences TLR-induced IL-12/IL-23 production.

In this study, we demonstrated that PIKfyve also has an important function in type I IFN production induced by TLR7/9. Apilimod treatment blocks TLR7/9-induced type I IFN production, as also observed in PIKfyve-deficient cells. However, the inhibitory effect is not mediated by the known role of PIKfyve in endosomal trafficking because TLR7/9 receptor and ligand trafficking is not impaired. Instead, we elucidated the downstream effector of PIKfyve in regulating type I IFN and IL-12p40 expression by inducing the expression of ATF3, thus unraveling the mechanism of this lipid kinase in modulating TLR signaling.

Materials and Methods

Constructs and reagents

The retrovirus constructs encoding TLR9-GFP and lentivirus mCherry-CD63 were made as previously described (6). pENTR-ATF3 (human) was purchased from Invitrogen and subcloned into pcDNA6.2-DEST.

All the control and gene-specific short hairpin RNAs (shRNAs) used in the study were ordered from Sigma-Aldrich MISSION shRNA collection. The nontarget shRNA is the pLKO.1-puro Non-Mammalian shRNA Control. This control contains a shRNA insert that does not target human and mouse genes. Phospho-p38, p38, phospho-p65, p65 and IκBα Abs were purchased from Cell Signaling Technology. ATF3 and IRAK1 Abs were obtained from Santa Cruz Biotechnology. FITC-CD11c and PE-B220 Abs were purchased from BD Pharmingen. Tubulin Ab was obtained from Abcam.

Novartis Institutes for Biomedical Research, Cambridge, MA 02139

[1]Current address: Pohang University of Science and Technology, Pohang, Republic of Korea

Received for publication September 9, 2013. Accepted for publication January 31, 2014.

The microarray datasets presented in this article have been submitted to the Gene Expression Omnibus (http://www.ncbi.nlm.nih.gov/geo/query/acc.cgi?acc=GSE22124) under accession number GSE22124.

Address correspondence and reprint requests to Dr. Qian Huang, Novartis Institutes for Biomedical Research, 500 Technology Square, Cambridge, MA 02139. E-mail address: qian.huang@novartis.com

The online version of this article contains supplemental material.

Abbreviations used in this article: ChIP, chromatin immunoprecipitation; ER, endoplasmic reticulum; pDC, plasmacytoid dendritic cell; PI(3)P, phosphatidylinositol 3-phosphate; $PI(3,5)P_2$, phosphatidylinositol 3,5-bisphosphate; qPCR, quantitative PCR; shRNA, short hairpin RNA; SLE, systemic lupus erythematosus.

CpG and ssRNA were synthesized by Integrated DNA Technologies using the following sequence: 5′-UUGUUGUUGUUGUU-3′ (poly-GU), 5′-GUUCCAUUGGCUCUGGUGCUU-3′ (STAT-2AS), 5′-TCCATGACGTTCCTGACGTT-3′ (ODN1826), 5′-GGGGGACGATCGTCGGGGGG-3′ (ODN2216), and 5′-GGTGCATCGATGCAGGGGGG-3′ (D19). Other TLR ligands were purchased from Invivogen.

Human IFN-α and mouse IFN-α/IFN-β ELISA kits were purchased from PBL. All other ELISA kits were obtained from R&D Systems. All quantitative PCR (qPCR) probes were purchased from ABI.

Virus production and infection

Lentivirus shRNA was packaged in 293T cells via cotransfection of pLP1, pLP2, and pLP/VSVG. Retrovirus was packaged in 293T cells via cotransfection of Gag-Pol and VSVG. RAW264.7 cells were infected with supernatant containing virus plus polybrene (final concentration, 8 μg/ml; Sigma-Aldrich) overnight. The stable cell lines were maintained in medium containing puromycin (6 μg/ml) or G418 (400 μg/ml).

Cell culture

RAW264.7 and 293T cells were purchased from American Type Culture Collection and maintained under standard conditions described in the American Type Culture Collection instructions. Human PBMCs were isolated using Ficoll (GE Health). Human pDCs were enriched from $CD3^+$-depleted PBMCs. Mouse pDCs were differentiated from mouse bone marrow cells, using Flt3L as previously described (18). pDC differentiation was confirmed by CD11c and B220 staining.

Mouse breeding

Mouse strains Vac14<*ingls*> and C57 BL/6 were purchased from The Jackson Laboratory. All mice were maintained according to Novartis Institutes for BioMedical Research animal guidelines.

Genome-wide gene expression analysis

Genome-wide gene expression analysis was performed as previously described (19). Briefly, RAW264.7 cells were treated with TLR ligand and compound. Cells were harvested at 0, 1, 3, 7, and 22 h. Total RNA was isolated and hybridized to mouse oligonucleotide arrays (Affymetrix). Data were collected and analyzed using Spotfire. Microarray datasets have been deposited into the Gene Expression Omnibus (http://www.ncbi.nlm.nih.gov/geo/query/acc.cgi?acc=GSE22124) under accession number GSE22124.

Intracellular pH measurement

The intracellular pH measurement was performed as described (20). Briefly, RAW264.7 cells were seeded into eight-well cover glass-bottom chambers (Lab-Tek) overnight. Cells were incubated with the LysoSensor Yellow/Blue dextran (1 mg/ml, Invitrogen) for 14 h and then washed with cold PBS. For the standard curve, medium was changed to pH standard buffer with 10 μM monensin and 20 μM nigericin. For the tested samples, medium was changed to assay medium (phenol red–free DMEM; 5% FBS; 25 mM HEPES, pH7.4) and incubated with compound for 60 min. Images were captured by Zeiss LSM510, using Plan-Apochromat ×63/1.4 oil differential interference contrast lens. The Yellow/Blue ratio images were processed and quantified with MetaXpress software. The standard curve was plotted according to the image ratio. The pH of lysosome in compound-treated cells was calculated based on the standard curve.

CpG uptake

The CpG uptake assay was performed as previously described (21).

Live cell imaging

For live cell imaging, cells were seeded into a P35 glass-bottom dish (MatTek) (4×10^5 cells per dish) and maintained in phenol red–free DMEM supplemented with 5% FBS and 25 mM HEPES (pH 7.4) at 37°C in an environment chamber. Images were acquired using a Zeiss LSM510 confocal microscope with a Plan-Apochromat ×63/1.4 oil differential interference contrast lens. Zeiss LSM Image Browser was used for imaging analysis.

Luciferase reporter assay

293T cells were seeded on 24-well plates for 16 h and transiently transfected with 50 ng firefly luciferase reporter plasmid, 1 ng *Renilla* luciferase plasmid, and 70 ng total of various expression vectors. The firefly and *Renilla* luciferase activities were measured using Dual-Glo Luciferase Assay System (Promega). The *Renilla* luciferase activity was used as an internal control for normalization.

Chromatin immunoprecipitation assay

RAW264.7 cells were cross-linked by 1% formaldehyde, and chromatin immunoprecipitation (ChIP) assay was performed according to the manufacturer's protocol (Millipore). A total of 10 μg ATF3 Abs (Santa Cruz Biotechnology) was used for immunoprecipitation. The purified DNA, after reverse cross-linking, was analyzed by real-time PCR, using primers specific for the promoters of IFN-β.

Sequences of promoter-specific primers: IFN-β, sense: 5′-GAGCTATGGCCCATTGATGT-3′; anti-sense: 5′-GCTGCTGCCCTTTGAAATAG-3′.

qPCR

For qPCR assay, mRNAs were isolated using the TurboCapture 96 mRNA Kit (QIAGEN). cDNAs were synthesized using the ABI High Capacity cDNA Reverse Transcription Kit. TaqMan Gene Expression Assays were performed using the ABI 7900HT Fast Real-Time PCR System. All data were normalized to β-actin.

Results

Inactivation of PIKfyve by apilimod selectively inhibits TLR-induced expression of type I IFN

Apilimod is the first clinically evaluated low m.w. IL-12/IL-23 antagonist that selectively blocks TLR-induced IL-12/IL-23 (16). Recently, we identified PIKfyve as the molecular target of apilimod in the antagonism of IL-12/IL-23 production (15). Apilimod is shown to be a potent and highly selective PIKfyve inhibitor. It has an IC_{50} of 14 nM against PIKfyve kinase in vitro without any activity toward other lipid kinases (15). Because PIKfyve is a key regulator of endosomal integrity, we decided to investigate its role in endosomal TLR signaling. We used global gene expression analysis in RAW264.7 cells treated with or without apilimod and stimulated with TLR7 agonist R848. Of interest, we found apilimod blocked the expression of only a subset of cytokines, which includes IFN-β, a member of the type I IFN family (GSE22124). This result was confirmed by both qPCR and ELISA assay (Fig. 1A). Moreover, apilimod also blocks TLR3- and TLR9-induced expression of IFN-β in RAW264.7 cells (Fig. 1B). The other type I IFN family member, IFN-α, is exclusively produced by TLR7/TLR9-stimulated pDCs. We found apilimod also blocked TLR9-induced production of IFN-α/β in mouse Flt3L pDCs and TLR7/TLR9-induced production of IFN-α in human pDCs (Fig. 1C, 1D). Although apilimod inhibited the expression of type I IFN, it did not inhibit TLR-induced TNF-α in mouse cells and IL-8 production in human pDCs (Fig. 1A, 1C, 1D). Apilimod thus selectively inhibits the expression of type I IFN across multiple endosomal TLR pathways.

To confirm that apilimod blocks production of type I IFN by inactivation of PIKfyve, we used the spontaneous mutant mouse, *ingls,* which carries a missense mutation in PIKfyve adaptor Vac14 (L156R) (9). The *Ingls* mutation interrupts the interaction of PIKfyve with Vac14, which abolishes the kinase activity of PIKfyve and reduces the level of $PI(3,5)P_2$. Indeed, the expression of both IFN-α and IFN-β was abolished following TLR9 activation in pDCs derived from $Vac14^{ingls/ingls}$ mice (Fig. 1E). These data suggest that PIKfyve is required for TLR-induced IFN-α production.

PIKfyve modulates the expression of TLR-induced type I IFN via mechanisms independent of receptor and ligand trafficking

Although PIKfyve is required for TLR-induced expression of type I IFN, the molecular mechanism is unknown. It has been shown that all type I IFN–inducing TLRs signal from the endolysosome (22). We hypothesized that intracellular TLR/ligand interaction may be compromised by PIKfyve inactivation because PIKfyve and its product $PI(3,5P)_2$ are regulators of endolysosome membrane

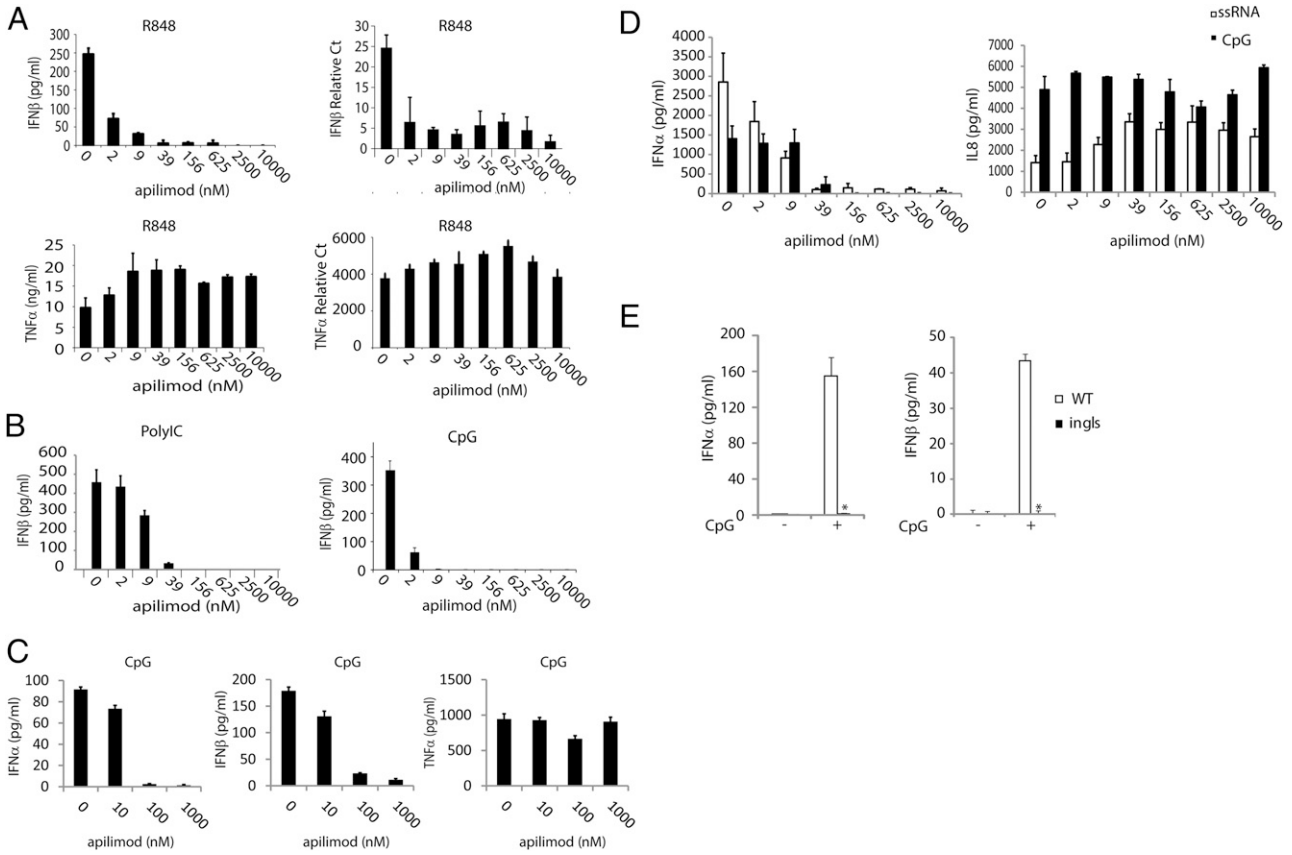

FIGURE 1. PIKfyve is required for TLR-induced type I IFN production. The production of cytokines was measured by ELISA following overnight stimulation. mRNAs were collected after 1 h of stimulation for determination of TNF-α and 4 h of stimulation for determination of IFN-β by qPCR. (**A** and **B**) RAW264.7 cells were treated with the indicated dose of apilimod in the presence of R848 (0.1 μM), polyinosinic-polycytidylic acid (100 μg/ml), or CpG (ODN1826, 5 μM). All bar graphs of IFN-β production were analyzed using one-way ANOVA ($p < 0.001$), indicating a significant effect of apilimod on the production of IFN-β. (**C**) Mouse Flt3L DCs were treated with the indicated dose of apilimod in the presence of CpG (D19, 5 μM). (**D**) Human pDCs were treated with the indicated dose of apilimod in the presence of ssRNA (poly-GU, 20 μg/ml, and packaged with DOTAP) or CpG (ODN2216, 5 μM). All bar graphs were analyzed using one-way ANOVA ($p < 0.0001$), indicating a significant effect of apilimod on the production of type I IFN. (**E**) Flt3L DCs from wild-type (WT) or *ingls* mice ($n = 3$) were challenged with type A CpG (D19, 5 μM) for 24 h. Representative results from experiments using three matched WT/*ingls* pairs. *$p < 0.05$ using Student *t* test. Data with error bars represent mean ± SD.

traffic (23); that is, inhibition of PIKfyve could affect endosomal pH or cause a defect in ligand or receptor translocation in endolysosomes.

To investigate the role of PIKfyve in endolysosome acidification, we measured the endolysosome pH using LysoSensor, a pH indicator exhibiting a pH-dependent fluorescence change. Although bafilomycin, an inhibitor of vacuolar-type H^+ ATPase, neutralized the endolysosomal pH, inactivation of PIKfyve by apilimod did not block endolysosomal acidification in RAW264.7 cells even at a concentration as high as 1 μM (Fig. 2A). Subsequently, we studied the effect of PIKfyve inhibition on intracellular trafficking of TLR9 and its ligand (CpG). Inhibition of PIKfyve did not disrupt CpG-induced endolysosomal localization of TLR9-GFP (Fig. 2B, Supplemental Fig. 1A, 1B), as a majority of TLR-GFP colocalized with endolysosomal marker (mCherry-CD63), but not ER marker (ER-mCherry), in the presence of apilimod. Inactivation of PIKfyve therefore does not disrupt ER–endolysosomal trafficking of TLR9. Moreover, we tested CpG uptake, using flow cytometry. PIKfyve inhibition had no effect on CpG uptake by cells (Fig. 2C). We also did not observe a major defect in CpG trafficking to endolysosomes in apilimod-treated cells, except a slight delay at the early stage, which did not lead to the inhibition of TNF-α production (Fig. 1A, Supplemental Fig. 1C).

Furthermore, intracellular distribution of a TLR7 agonist R848 over endolysosomes was not disrupted in the presence of apilimod (Fig. 2D; TLR9-GFP was used as a surrogate TLR7 marker because TLR7-GFP could not be visualized in living cells). Of note, R848 accumulation appeared to increase in endolysosomes, which is consistent with increased activation of NF-κB and p38 upon apilimod treatment, as well as enhanced expression of TNF-α in RAW264.7 cells (Fig. 1A, 2E). Therefore, it appears that inactivation of PIKfyve lipid kinase activity selectively inhibits the expression of type I IFN by mechanism(s) independent of ligand/receptor trafficking.

Inactivation of PIKfyve induces expression of the transcription repressor ATF3

To explore the underlying mechanism of PIKfyve-dependent control of cytokine expression, we used global gene expression analysis. We focused on R848 stimulation, as we did not observe any defect of its accumulation in endolysosomes. It appears that newly synthesized protein(s) might be required for the PIKfyve inactivation–mediated cytokine silencing effect, because R848-induced late responsive genes are more sensitive to apilimod treatment (Fig. 3A and GSE22124). Indeed, cycloheximide, an inhibitor of protein biosynthesis, blocked the apilimod-mediated silencing and rescued production of IFN-β (Fig. 3B). A known transcriptional repressor for TLR-induced IL-12p40, ATF3 was among the most strongly upregulated genes in response to apilimod and R848 stimulation (Fig. 3C and GSE22124) (24, 25). Both

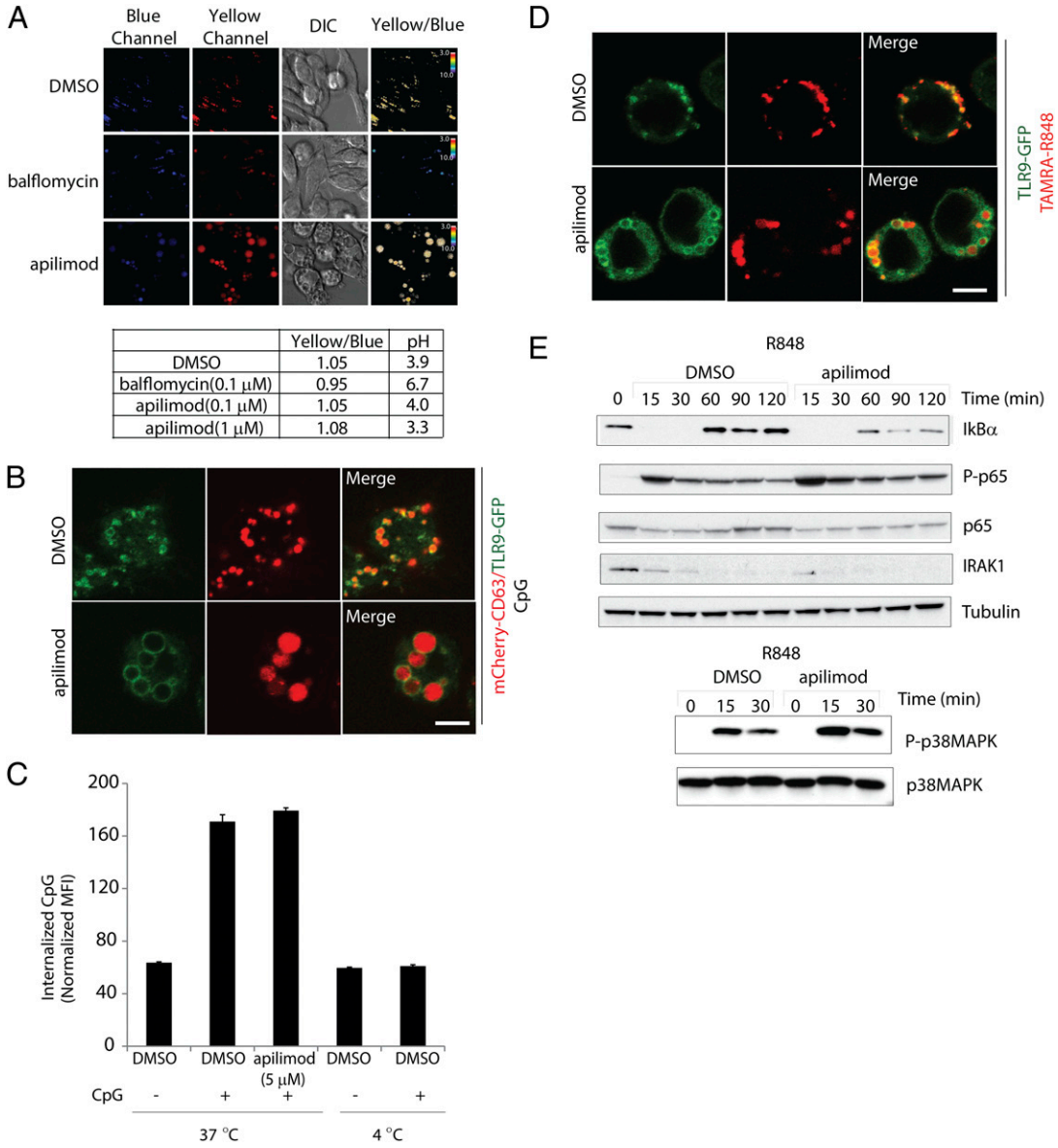

	Yellow/Blue	pH
DMSO	1.05	3.9
balflomycin(0.1 μM)	0.95	6.7
apilimod(0.1 μM)	1.05	4.0
apilimod(1 μM)	1.08	3.3

FIGURE 2. PIKfyve modulates the expression of TLR-mediated type I IFN via mechanisms independent of receptor and ligand trafficking. (**A**) Intracellular pH measurement: RAW264.7 cells were incubated with LysoSensor Yellow/Blue dextran and treated with bafilomycin (0.1 μM) or apilimod (0.1 μM or 1 μM). The yellow channel was displayed as a red color. The pH measurement is derived from the Yellow/Blue ratio. (**B**) RAW264.7 cells stably expressing TLR9-GFP and mCherry-CD63 were treated with DMSO or apilimod (100 nM) in the presence of CpG (ODN1826, 5 μM) for 60 min. Scale bar, 5 μm. Cells were imaged using Zeiss LSM510 confocal microscopy with a ×63 lens. (**C**) RAW264.7 cells were treated with DMSO or apilimod at the indicated temperature and fed with FITC-CpG (ODN1826, 2 μM) for 30 min. Trypan blue was added to quench the exogenous FITC-CpG for 5 min. Cells were washed three times with PBS. The internalized CpG was measured by flow cytometry. Data with error bars represent mean ± SD. (**D**) RAW264.7 cells stably expressing TLR9-GFP (surrogate TLR7 marker) were treated with DMSO or apilimod (100 nM) in the presence of TAMRA-R848 (5 μM) for 120 min. Cells were washed once before imaging. Scale bar, 5 μm. Cells were imaged using Zeiss LSM510 confocal microscopy with a ×63 lens. (**E**) RAW264.7 cells were pretreated with DMSO or apilimod (100 nM) for an hour and then stimulated with R848 (0.1 μM). Cells were lysed at the indicated times and blotted with the indicated Abs. Representative results from two independent experiments.

ATF3 mRNA and protein expression were greatly induced by apilimod in RAW264.7 cells (Fig. 3D and Supplemental Fig. 2A, 2B), as well as in Flt3L DCs treated with apilimod or Flt3L DCs isolated from Vac14 mutant mice (Fig. 3E, 3F). Our data suggest that ATF3 is specifically induced upon inactivation of PIKfyve.

PIKfyve inhibitor silences cytokine production by induction of ATF3

Next, we set out to examine whether the induction of ATF3 by PIKfyve inactivation plays a role in the effect of apilimod on cytokine expression. Although repression of TLR-induced IL-12p40 production by ATF3 has been reported (24, 25), its effect on type I IFN expression is unknown. To determine the role of ATF3 in this process, we established an IRF7-dependent IFN-β promoter reporter system in 293T cells. Overexpression of ATF3 suppressed IRF7-driven IFN-β promoter activation in a dose-dependent manner (Fig. 4A). In contrast, MyD88-driven activation of the NF-κB–dependent ELAM promoter was intact when cells were cotransfected with ATF3. ATF3 may thus function as a specific repressor of the IFN-β promoter. In addition, silencing of ATF3 also rescued the inhibitory effect of apilimod on R848-induced expression of IFN-β but had little effect on induction of TNF-α by R848 (Fig. 4B, 4C). PIKfyve inactivation may thus selectively inhibit IFN-β expression via induction of ATF3. Furthermore,

A

R848		
Time	Upregulated genes	Inhibited by apilimod (%)
1hr	58	2
3hr	380	26
7hr	497	49
22hr	417	34

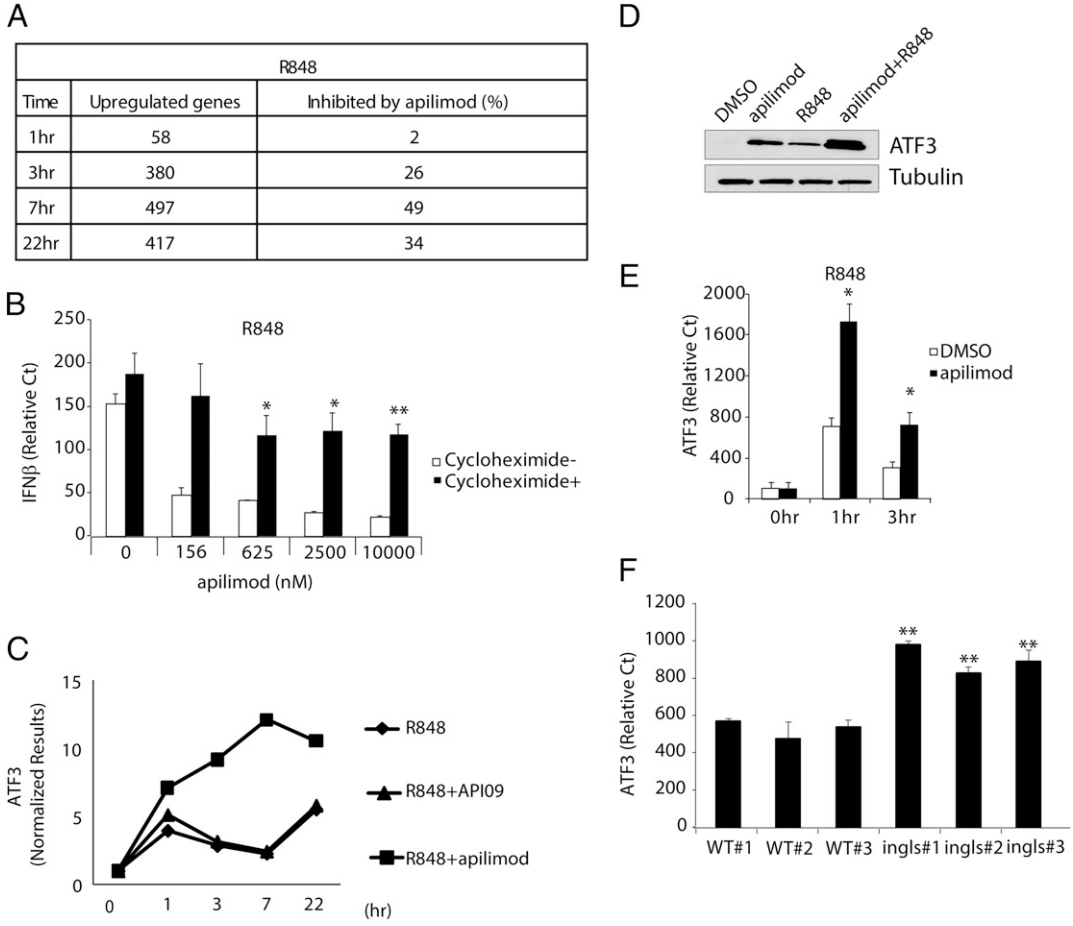

FIGURE 3. Inactivation of PIKfyve induces expression of the transcription repressor ATF3. (**A**) Analysis of global gene expression in RAW264.7 cells challenged with R848 (0.1 μM) in the presence of apilimod (1 μM) at the indicated times. Upregulated genes were defined as the gene whose induction over DMSO control ≥2-fold. (**B**) RAW264.7 cells were pretreated with cycloheximide (20 μg/ml) or DMSO for 30 min before being incubated with the indicated dose of apilimod and R848 (0.1 μM). The mRNAs were collected at 4 h for qPCR assay. $*p < 0.1$, $**p < 0.01$. (**C**) Kinetics of ATF3 mRNA expression in RAW264.7 cells treated with apilimod (1 μM) or API09 (15) (1 μM, inactive analog of apilimod) in the presence of R848 (0.1 μM). (**D**) RAW264.7 cells were treated with apilimod (1 μM) and R848 (0.1 μM) for 4 h. Cells were lysed and blotted with indicated Abs. (**E**) Flt3L DCs were treated with DMSO or apilimod (1 μM) and stimulated with R848 (10 μM). mRNAs were collected at the indicated times for qPCR. $*p < 0.1$. (**F**) Flt3L DCs from wild-type or *ingls* mice were challenged with R848 (10 μM). mRNAs were collected at 4 h for qPCR. $**p < 0.01$. Data with error bars represent mean ± SD.

knockdown of ATF3 antagonized the inhibitory effect of apilimod on expression of IL-12p40 in THP-1 cells (Supplemental Fig. 3), which also confirms that ATF3 is required for PIKfyve-mediated IL-12p40 expression. Therefore, inactivation of PIKfyve promotes ATF3 expression and potentiates ATF3-mediated silencing of a subset of cytokine expression.

To gain mechanistic insights into ATF3-dependent regulation of cytokine expression mediated by PIKfyve inactivation, we examined the binding of ATF3 to the promoter of IFN-β upon R848 stimulation in the presence or absence of apilimod by ChIP. As shown in Fig. 4D, R848-induced ATF3 was recruited to the IFN-β promoter, suggesting ATF3 might play a negative regulatory role in IFN-β expression, as observed with IL-12p40 (24, 25). Of interest, significantly more ATF3 bound to the IFN-β promoter when cells were treated with apilimod. These data confirm that PIKfyve inactivation regulates the expression of IFN-β via ATF3 modulation. In summary, apilimod enhances TLR-induced ATF3 expression and promotes occupancy of ATF3 on the IFN-β promoter, and in turn silences its expression.

Discussion

In this study, we demonstrated that PIKfyve is required for endosomal TLR-induced type I IFN production. Surprisingly, despite the induction of massive vacuoles from endosome/lysosome origin in cells when PIKfyve is inactivated, TLR7/TLR9 receptor and ligand trafficking and activation in endolysomes appear to be normal. This unexpected finding led to the discovery of a mechanism by which PIKfyve exerts its cellular function via induction of the transcription repressor ATF3. Moreover, we uncovered a previously unknown function of ATF3 in regulating type I IFN expression. Our results thus suggest a new druggable node for selective regulation of TLR-induced type I IFN expression, and in turn, provide opportunities for pharmacological intervention in IFN-α–mediated diseases.

Human IFN-α is exclusively produced by pDCs following activation of endolysosomal TLR7/TLR9. Although IFN-α plays a critical role in antiviral responses, multiple lines of evidence suggest that abnormal upregulation of IFN-α contributes to the progression of SLE. To date, a number of approaches are being evaluated in the clinic by targeting IFN-α, including the administration of anti–IFN-α Ab in lupus patients (26). Besides biological therapy, an orally available selective small-molecule IFN-α antagonist will be highly desirable. In our study, we found that apilimod, a clinically evaluated PIKfyve antagonist, selectively blocks TLR7/TLR9-induced IFN-α in pDCs. This approach provides an advantage over the IFN-α Ab by blocking the IFN-α

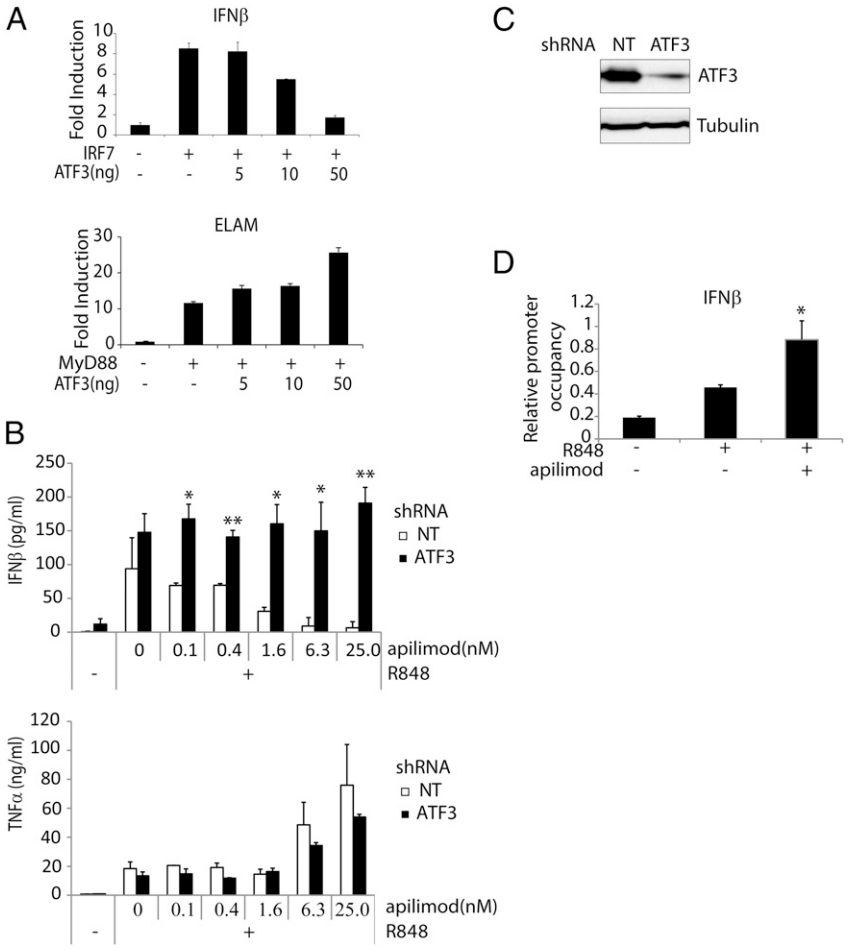

FIGURE 4. PIKfyve inhibitor silences IFN-β production by induction of ATF3. (**A**) 293T cells were transfected with a reporter plasmid containing IFN-β or ELAM promoter and other indicated plasmids for 48 h. The reporter activation was measured by a Dual-Glo Luciferase Assay. The results were normalized with those from *Renilla* luciferase. $p < 0.001$ for the IFN-β promoter results by one-way ANOVA. (**B**) RAW264.7 cells stably expressing the indicated shRNAs were treated with increasing doses of apilimod in the presence or absence of R848 (0.1 μM). Cell supernatants were collected following 18 h of stimulation for ELISA. $*p < 0.05$, $**p < 0.01$. (**C**) RAW264.7 cells stably expressing nontarget or ATF3 shRNAs were treated with R848 (0.1 μM) and apilimod (100 nM). Cells were lysed at 4 h and blotted with the indicated Abs. (**D**) RAW264.7 cells were treated with DMSO or apilimod (1 μM) and stimulated with R848 (0.1 μM) for 4 h. Recruitment of ATF3 to the indicated promoters was measured by ChIP assay. $*p < 0.1$, indicating a significant difference on the recruitment of ATF3 between R848- and R848/apilimod-treated samples. Data with error bars represent mean ± SD.

pathway relevant to disease progression. Therefore, these results shed light on a novel approach for SLE treatment.

Despite the induction of vacuoles, trafficking and activation of TLR7/TLR9 receptors and their reported ligands appear to be normal. The PIKfyve inhibitor only slightly delays the CpG trafficking from early endosomes to endolysosomes, but does not block ligand–receptor interaction in endolysosomes at later stages in RAW264.7 cells. It has been reported that CpG uptake is impaired in RAW264.7 cells that express the VPS34 kinase–dead mutant (27). VPS34 is a class III PI3K that phosphorylates the D-3 position on PI to yield PI(3)P. PI(3)P and PI(3,5)P_2 might thus regulate distinct steps of intracellular trafficking of CpG. CpG could use an alternative trafficking route independent of MVB, as supported by the observation that CpG could still reach the endolysosomal compartment at a later stage in the presence of PIKfyve inhibitors.

TLR9 translocates normally to endolysosomes, despite the enlargement of both endosomes and lysosomes when PIKfyve activity is inhibited. Although PIKfyve is required for retrograde trafficking from lysosomes to the trans–Golgi network (28), its activity may not be required for the cargo trafficking from the trans–Golgi network to endolysosomes, as proposed for translocation of TLR9 from the ER (29).

Importantly, using apilimod as a tool, we shed light on the intracellular trafficking of R848, a small-molecule TLR7/TLR8 pathway activator. We showed that R848 was localized to endolysosomes in live cells and that its trafficking is PIKfyve independent. More R848 accumulates within endolysosomes in the presence of apilimod (Fig. 2D), possibly owing to the enlarged size of endolysosomes or defects of exit, which might explain the increase of TNF-α production following overnight treatment with apilimod (Fig. 1A) and sustained activation of signaling events downstream of TLR7 (Fig. 2E). R848 might enter the cell in a clathrin-independent manner, via interaction with other protein(s) or accumulation in acidic endolysosomes as a weak base. Our results therefore suggest further specialization in the endolysosomal handling of the nucleic acid–sensing TLR to an extent greater than has been appreciated until now.

How can an endosomal lipid kinase modulate the activation of only a subset of cytokines downstream of TLR7 and TLR9? Although apilimod reportedly inhibited IL-12p40 expression by blocking translocation of c-Rel to the nucleus (30), we failed to detect this defect in IFN-γ/LPS stimulated THP-1 cells in the presence of apilimod (Supplemental Fig. 4). Subsequently, we identify the induction of ATF3 as the mechanism by which PIKfyve inhibitors exert their endocytosis-independent function and selectively inhibit IL-12p40 and type I IFN expression. Apilimod treatment strongly enhanced expression of ATF3 in response to TLR engagement and amplified the ATF3-mediated adaptive gene–silencing mechanism. Although ATF3 might be induced by Ca^{2+} imbalance in the ER (31), we did not observe any signs of ER stress induced upon apilimod treatment, determined by analysis of the activation of all three branches of the unfolded protein response (data not shown). Therefore, it is unlikely that ATF3 is induced by a systemic stress response. Instead, an imbalance of PI(3)P/PI(3,5)P_2 in endolysosomal membranes induced by inactivation of PIKfyve may trigger activation of an unknown endolysosomal lipid sensor, which leads to a specific induction of ATF3.

In summary, we uncover a new role for PIKfyve in selectively regulating TLR-induced type I IFN. Of interest, TLR7/TLR9 re-

ceptor and ligand trafficking and activation in endolysomes appear to be normal when PIKfyve is inactivated. This finding led to the discovery of a mechanism by which PIKfyve exerts its novel cellular function via induction of a transcriptional repressor ATF3. Our study thus couples a specific phosphoinositide composition in endolysosomes with a negative feedback loop in TLR signaling.

Acknowledgments

We thank J. Schustak for performing the human pDC assay, I. Cornella-Taracido and E. Harrington for synthesizing TAMRA-R848, J. Vyas (Massachusetts General Hospital) for providing mCherry-CD63 construct, A.T. Maniatis (Columbia University) for providing IFN-β promoter construct, N. Hartmann for performing Affymetrix microarray profiling, A. Ho and A. Szilvasi for providing assistance in imaging and flow cytometry, and A. Titelbaum for lending assistance in mouse breeding.

Disclosures

Except for Y.-M.K., all authors are employees of Novartis Institutes for Biomedical Research. Novartis is not involved in the discovery and development of apilimod.

References

1. Takeuchi, O., and S. Akira. 2010. Pattern recognition receptors and inflammation. *Cell* 140: 805–820.
2. Krieg, A. M., and J. Vollmer. 2007. Toll-like receptors 7, 8, and 9: linking innate immunity to autoimmunity. *Immunol. Rev.* 220: 251–269.
3. Rönnblom, L., and G. V. Alm. 2002. The natural interferon-alpha producing cells in systemic lupus erythematosus. *Hum. Immunol.* 63: 1181–1193.
4. Schmidt, K. N., and W. Ouyang. 2004. Targeting interferon-alpha: a promising approach for systemic lupus erythematosus therapy. *Lupus* 13: 348–352.
5. Latz, E., A. Schoenemeyer, A. Visintin, K. A. Fitzgerald, B. G. Monks, C. F. Knetter, E. Lien, N. J. Nilsen, T. Espevik, and D. T. Golenbock. 2004. TLR9 signals after translocating from the ER to CpG DNA in the lysosome. *Nat. Immunol.* 5: 190–198.
6. Kim, Y. M., M. M. Brinkmann, M. E. Paquet, and H. L. Ploegh. 2008. UNC93B1 delivers nucleotide-sensing toll-like receptors to endolysosomes. *Nature* 452: 234–238.
7. Gilliet, M., W. Cao, and Y. J. Liu. 2008. Plasmacytoid dendritic cells: sensing nucleic acids in viral infection and autoimmune diseases. *Nat. Rev. Immunol.* 8: 594–606.
8. Shisheva, A. 2008. PIKfyve: Partners, significance, debates and paradoxes. *Cell Biol. Int.* 32: 591–604.
9. Jin, N., C. Y. Chow, L. Liu, S. N. Zolov, R. Bronson, M. Davisson, J. L. Petersen, Y. Zhang, S. Park, J. E. Duex, et al. 2008. VAC14 nucleates a protein complex essential for the acute interconversion of PI3P and PI(3,5)P(2) in yeast and mouse. *EMBO J.* 27: 3221–3234.
10. Zhang, Y., S. N. Zolov, C. Y. Chow, S. G. Slutsky, S. C. Richardson, R. C. Piper, B. Yang, J. J. Nau, R. J. Westrick, S. J. Morrison, et al. 2007. Loss of Vac14, a regulator of the signaling lipid phosphatidylinositol 3,5-bisphosphate, results in neurodegeneration in mice. *Proc. Natl. Acad. Sci. USA* 104: 17518–17523.
11. Chow, C. Y., Y. Zhang, J. J. Dowling, N. Jin, M. Adamska, K. Shiga, K. Szigeti, M. E. Shy, J. Li, X. Zhang, et al. 2007. Mutation of FIG4 causes neurodegeneration in the pale tremor mouse and patients with CMT4J. *Nature* 448: 68–72.
12. Ikonomov, O. C., D. Sbrissa, K. Mlak, and A. Shisheva. 2002. Requirement for PIKfyve enzymatic activity in acute and long-term insulin cellular effects. *Endocrinology* 143: 4742–4754.
13. Jefferies, H. B., F. T. Cooke, P. Jat, C. Boucheron, T. Koizumi, M. Hayakawa, H. Kaizawa, T. Ohishi, P. Workman, M. D. Waterfield, and P. J. Parker. 2008. A selective PIKfyve inhibitor blocks PtdIns(3,5)P(2) production and disrupts endomembrane transport and retroviral budding. *EMBO Rep.* 9: 164–170.
14. Ferguson, C. J., G. M. Lenk, and M. H. Meisler. 2009. Defective autophagy in neurons and astrocytes from mice deficient in PI(3,5)P2. *Hum. Mol. Genet.* 18: 4868–4878.
15. Cai, X., Y. Xu, A. K. Cheung, R. C. Tomlinson, A. Alcázar-Román, L. Murphy, A. Billich, B. Zhang, Y. Feng, M. Klumpp, et al. 2013. PIKfyve, a class III PI kinase, is the target of the small molecular IL-12/IL-23 inhibitor apilimod and a player in Toll-like receptor signaling. *Chem. Biol.* 20: 912–921.
16. Wada, Y., R. Lu, D. Zhou, J. Chu, T. Przewloka, S. Zhang, L. Li, Y. Wu, J. Qin, V. Balasubramanyam, et al. 2007. Selective abrogation of Th1 response by STA-5326, a potent IL-12/IL-23 inhibitor. *Blood* 109: 1156–1164.
17. Wada, Y., I. Cardinale, A. Khatcherian, J. Chu, A. B. Kantor, A. B. Gottlieb, N. Tatsuta, E. Jacobson, J. Barsoum, and J. G. Krueger. 2012. Apilimod inhibits the production of IL-12 and IL-23 and reduces dendritic cell infiltration in psoriasis. *PLoS ONE* 7: e35069.
18. Gilliet, M., A. Boonstra, C. Paturel, S. Antonenko, X. L. Xu, G. Trinchieri, A. O'Garra, and Y. J. Liu. 2002. The development of murine plasmacytoid dendritic cell precursors is differentially regulated by FLT3-ligand and granulocyte/macrophage colony-stimulating factor. *J. Exp. Med.* 195: 953–958.
19. Brogdon, J. L., Y. Xu, S. J. Szabo, S. An, F. Buxton, D. Cohen, and Q. Huang. 2007. Histone deacetylase activities are required for innate immune cell control of Th1 but not Th2 effector cell function. *Blood* 109: 1123–1130.
20. Chen, Q. R., L. Zhang, P. W. Luther, and A. J. Mixson. 2002. Optimal transfection with the HK polymer depends on its degree of branching and the pH of endocytic vesicles. *Nucleic Acids Res.* 30: 1338–1345.
21. Ishii, K. J., F. Takeshita, I. Gursel, M. Gursel, J. Conover, A. Nussenzweig, and D. M. Klinman. 2002. Potential role of phosphatidylinositol 3 kinase, rather than DNA-dependent protein kinase, in CpG DNA-induced immune activation. *J. Exp. Med.* 196: 269–274.
22. Kagan, J. C., T. Su, T. Horng, A. Chow, S. Akira, and R. Medzhitov. 2008. TRAM couples endocytosis of Toll-like receptor 4 to the induction of interferon-beta. *Nat. Immunol.* 9: 361–368.
23. Dove, S. K., K. Dong, T. Kobayashi, F. K. Williams, and R. H. Michell. 2009. Phosphatidylinositol 3,5-bisphosphate and Fab1p/PIKfyve underPPIn endolysosome function. *Biochem. J.* 419: 1–13.
24. Gilchrist, M., V. Thorsson, B. Li, A. G. Rust, M. Korb, J. C. Roach, K. Kennedy, T. Hai, H. Bolouri, and A. Aderem. 2006. Systems biology approaches identify ATF3 as a negative regulator of Toll-like receptor 4. *Nature* 441: 173–178.
25. Whitmore, M. M., A. Iparraguirre, L. Kubelka, W. Weninger, T. Hai, and B. R. Williams. 2007. Negative regulation of TLR-signaling pathways by activating transcription factor-3. *J. Immunol.* 179: 3622–3630.
26. McBride, J. M., J. Jiang, A. R. Abbas, A. Morimoto, J. Li, R. Maciuca, M. Townsend, D. J. Wallace, W. P. Kennedy, and J. Drappa. 2012. Safety and pharmacodynamics of rontalizumab in patients with systemic lupus erythematosus: results of a phase I, placebo-controlled, double-blind, dose-escalation study. *Arthritis Rheum.* 64: 3666–3676.
27. Kuo, C. C., W. T. Lin, C. M. Liang, and S. M. Liang. 2006. Class I and III phosphatidylinositol 3′-kinase play distinct roles in TLR signaling pathway. *J. Immunol.* 176: 5943–5949.
28. Ikonomov, O. C., D. Sbrissa, K. Mlak, R. Deeb, J. Fligger, A. Soans, R. L. Finley, Jr., and A. Shisheva. 2003. Active PIKfyve associates with and promotes the membrane attachment of the late endosome-to-trans-Golgi network transport factor Rab9 effector p40. *J. Biol. Chem.* 278: 50863–50871.
29. Ewald, S. E., B. L. Lee, L. Lau, K. E. Wickliffe, G. P. Shi, H. A. Chapman, and G. M. Barton. 2008. The ectodomain of Toll-like receptor 9 is cleaved to generate a functional receptor. *Nature* 456: 658–662.
30. Burakoff, R., C. F. Barish, D. Riff, R. Pruitt, W. Y. Chey, F. A. Farraye, I. Shafran, S. Katz, C. L. Krone, M. Vander Vliet, et al. 2006. A phase 1/2A trial of STA 5326, an oral interleukin-12/23 inhibitor, in patients with active moderate to severe Crohn's disease. *Inflamm. Bowel Dis.* 12: 558–565.
31. Spohn, D., O. G. Rössler, S. E. Philipp, M. Raubuch, S. Kitajima, D. Griesemer, M. Hoth, and G. Thiel. 2010. Thapsigargin induces expression of activating transcription factor 3 in human keratinocytes involving Ca2+ ions and c-Jun N-terminal protein kinase. *Mol. Pharmacol.* 78: 865–876.